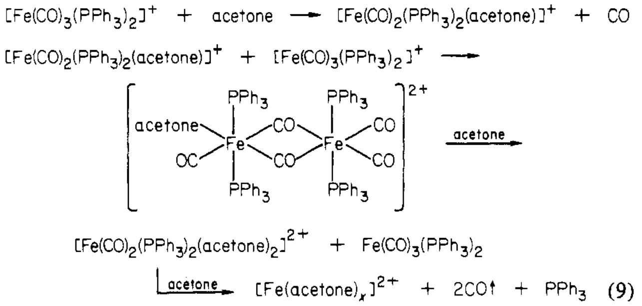
(9)

The observation of an ESR signal attributable to the intermediate $Fe(CO)_3(PPh_3)_2Cl$ at a considerable time after reaction of $[Fe(CO)_3(PPh_3)_2]^+$ with iron carbonyl complexes and some ligands is also consistent with dimer formation being associated with the reaction scheme. For example, dimers such as $[Rh(CO)_2(PPh_3)_2]_2$ and $[Rh(CO)(PPh_3)_2S]_2$ (S = solvent) react with $CHCl_3$ and CCl_4 to form $RhCl(CO)(PPh_3)_2$ via radical pathways.[20] The work of Connelly et al.[8,11] in conjunction with our studies and oxidative-addition reactions show that reactions of 17-electron radical cations of iron carbonyl compounds may proceed by a number of pathways. Reaction pathways may be parallel, and their characterization is correspondingly difficult.

Acknowledgment. This work was made possible by financial assistance from the Australian Research Grants Committee and the Deakin University Research Committee. We express our gratitude to both these committees for their support.

Registry No. *trans*-$Fe(CO)_3(PPh_3)_2$, 21255-52-7; *trans*-$[Fe(CO)_3(PPh_3)_2]PF_6$, 73979-30-3; $[Fe(CO)_3(PPh_3)_2]^+$, 60243-26-7; $Fe(CO)_4PPh_3$, 35679-07-3; $Fe(CO)_3(AsPh_3)_2$, 20516-72-7; $Fe(CO)_4AsPh_3$, 35644-25-8; $Fe(CO)_3(SbPh_3)_2$, 20516-73-8; $Fe(CO)_4SbPh_3$, 35917-16-9; $Fe(CO)_3(PPh_3)_2Cl$, 73979-38-1; CH_2Cl_2, 75-09-2; Pt, 7440-06-4; Ag, 7440-22-4; Hg, 7439-97-6; PPh_3, 603-35-0; $AsPh_3$, 603-32-7; $SbPh_3$, 603-36-1; acetone, 67-64-1; acetonitrile, 75-05-8.

---

[20] B. L. Booth, G. C. Casey, and R. N. Haszeldine, *J. Organomet. Chem.*, **224**, 197 (1982).

Contribution from the Department of Chemistry, University of Missouri—Rolla, Rolla, Missouri 65401,
Atomic Energy Research Establishment, Harwell, Didcot, OX11 0RA, England,
and Inorganic Chemistry and Chemical Crystallography Laboratories, Oxford University, Oxford, OX1 3PD, England

Study of the Iron–Phosphorus–Oxygen System by Mössbauer Effect, Neutron Diffraction, Magnetic Susceptibility, and Analytical Electron Microscopy: Some Pitfalls and Solutions in the Analysis of a Complex Mixture

GARY J. LONG,* ANTHONY K. CHEETHAM, and PETER D. BATTLE*

Received September 27, 1982

A sample of $FePO_4$ has been characterized by powder X-ray and neutron diffraction techniques, Mössbauer spectroscopy, magnetic susceptibility, and analytical electron microscopy. The analysis by diffraction methods is misleading and indicates that the sample is pure, but analytical electron microscopy shows that the material is triphasic and contains, in addition to $FePO_4$, a glassy component of approximate composition $Fe_3P_5O_{17}$ and a small amount of $Fe_7(PO_4)_6$, a mixed valence compound. The Mössbauer-effect spectra indicate that the material contains approximately 30% of the glass and approximately 2% of $Fe_7(PO_4)_6$. The Mössbauer spectra give the expected results for $FePO_4$ and confirm that it orders magnetically at 23.8 K. The glassy component orders at ca. 7 K, whereas $Fe_7(PO_4)_6$ remains paramagnetic down to ca. 10 K. The magnetic susceptibility data show ordering of $FePO_4$ and the glassy component at 24 and ca. 7 K, respectively. The combination of these various techniques has permitted a detailed description of this complex mixture.

Introduction

The discovery of novel ferrimagnetic properties in the isostructural compounds iron(III) sulfate[1] and iron(III) molybdate[2] led us to undertake a detailed study of the magnetic properties of iron(III) phosphate.[3] The latter compound adopts the berlinite ($AlPO_4$) structure,[4] which is related to that of α-quartz with each iron and phosphorus atom tetrahedrally bonded to four oxygen atoms. Prior to our work, little was known about the magnetic nature of iron(III) phosphate. Mössbauer-effect studies[5,6] had indicated that it is antiferromagnetic below ca. 25 K and exhibits a change in the sign of the quadrupole shift at ca. 18 K, but no magnetic susceptibility or neutron diffraction work had been reported. Our study revealed that it undergoes a unique spin-reorientation transition at ca. 17 K.[3]

Our initial measurements were hampered by impurities that were undetected in our characterization of the material by powder X-ray and neutron diffraction, but the combined use of the Mössbauer-effect, analytical electron microscopy, and magnetic susceptibility techniques has allowed us to resolve the detailed nature of the phases present. The purpose of this paper is to discuss the pitfalls that may be encountered when samples are evaluated by diffraction techniques and to describe the experiments that were used to elucidate the actual constituents of the mixture.

Experimental Section

Molten, commercial grade $FePO_4$ (Merck) was held at 1000 °C for 4 h in an open platinum crucible before quenching to room temperature.

The Mössbauer-effect spectra of the ground product were obtained on a Harwell constant-acceleration spectrometer[1] that utilized a room-temperature rhodium-matrix source and was calibrated with room-temperature natural α-iron foil. Spectra obtained at 4.2 K and below were measured in a cryostat in which the sample was placed

---

* To whom correspondence should be addressed: G.J.L., University of Missouri—Rolla; P.D.B., Oxford University.

[1] Long, G. J.; Longworth, G.; Battle, P.; Cheetham, A. K.; Thundathil, R. V.; Beveridge, D. *Inorg. Chem.* **1979**, *18*, 624.
[2] Battle, P. D.; Cheetham, A. K.; Long, G. J.; Longworth, G. *Inorg. Chem.* **1982**, *21*, 4223.
[3] Battle, P. D.; Cheetham, A. K.; Gleitzer, C.; Harrison, W. T. A.; Long, G. J.; Longworth, G. *J. Phys. C.* **1982**, *15*, L919.
[4] Ng, H. N.; Calvo, C. *Can. J. Chem.* **1975**, *53*, 2064.
[5] Bruckner, W.; Fuchs, W.; Ritter, G. *Phys. Lett. A* **1967**, *26A*, 32.
[6] Beckmann, V.; Bruckner, W.; Fuchs, W.; Ritter, G.; Wegener, H. *Phys. Status Solidi* **1968**, *29*, 781.

0020-1669/83/1322-3012$01.50/0

Table I. Room-Temperature Coordinates for $FePO_4$ Derived from Neutron Diffraction Results

	x		y		z	
atom	this work	ref 4	this work	ref 4	this work	ref 4
Fe	0.4550 (7)	0.4583 (3)	0	0	$^1/_3$	$^1/_3$
P	0.4614 (13)	0.4577 (6)	0	0	$^5/_6$	$^5/_6$
O1	0.4217 (13)	0.419 (2)	0.3153 (8)	0.318 (1)	0.3970 (2)	0.3963 (4)
O2	0.4081 (13)	0.413 (2)	0.2612 (9)	0.264 (1)	0.8759 (3)	0.8749 (5)

Table II. Mössbauer-Effect Spectral Data for the Paramagnetic Phase[a]

	$FePO_4$				$Fe_3P_5O_{17}$ (glassy component)				$Fe_7(PO_4)_6$			
T, K	δ	ΔE_Q	Γ	%A	δ	ΔE_Q	Γ	%A	δ	ΔE_Q	Γ	%A
300	0.30	0.62	0.33	78.8	0.39	1.05	0.38	18.2	1.17	2.56	0.56	3.0
78	0.39	0.63	0.33	75.6	0.48	1.05	0.42	20.8	1.16	2.79	0.62	3.6
44.5	0.39	0.62	0.31	77.4	0.48	1.06	0.41	20.8	1.19	2.80	0.46	1.8
30.0	0.39	0.63	0.32	69.6	0.49	1.04	0.43	20.7	1.20	2.80	0.34	1.4
25.0	0.39	0.62	0.31	73.8	0.48	1.02	0.46	24.1	1.20[b]	2.80[b]	0.45	2.1
24.6	0.39	0.62	0.34	80.0	0.48	1.07	0.38	18.4	1.20[b]	2.80[b]	0.45	1.5
24.4	0.39	0.62	0.31	67.9	0.49	0.99	0.53	29.9	1.20[b]	2.80[b]	0.45	2.2
23.8	0.39	0.62	0.36	50.5	0.48	0.99	0.38	16.2	1.20	2.77	0.40	2.0

[a] All data in mm/s relative to room-temperature natural α-iron foil. [b] Constrained values.

directly in the liquid helium. Temperatures between 4.2 and 78 K were obtained through the use of a variable-temperature insert placed in the liquid-helium cryostat. The temperature was measured by a gold–iron thermocouple and was controlled to ±0.1 K. The magnetically perturbed spectra were obtained with a British Oxygen Corp. superconducting magnet and cryostat which produced a transverse applied magnetic field. The Mössbauer spectra were evaluated by using least-squares minimization techniques and the Harwell IBM 370/168 computer facilities. The magnetic susceptibility results were obtained on an Oxford Instruments Faraday balance by using an applied field of 9.95 kG and a magnetic field gradient of 122 G/cm. X-ray emission microanalytical spectra and electron diffraction patterns were obtained on a JEOL 100CX TEMSCAN analytical electron microscope.[7] The X-ray emission spectra were measured at 100 keV, and the iron to phosphorus ratio was obtained by using the ratio method[8] with the intensities of the phosphorus K$\alpha\beta$ and the iron Kα lines. The proportionality constant, $k_{Fe/P}$, was determined from four standard materials, $FePO_4$, Fe_2PO_5, Fe_3PO_7, and Fe_9PO_{12}, which were characterized by chemical analysis and single-crystal X-ray methods. The respective ratios are plotted in Figure 1 and yield a linear relationship, with a slope of 0.6075, an intercept of 0.0295, and a correlation coefficient of 0.999, that is in good agreement with the thin-crystal approximation.[8]

Room-temperature powder neutron diffraction data were recorded on the Curran diffractometer at A.E.R.E., Harwell, by using a mean neutron wavelength of 1.37 Å and a monitor count of 3.3×10^4 neutrons per step.

Results

The X-ray and neutron (Figure 2) powder diffraction patterns contain only reflections due to the berlinite structure of $FePO_4$, and a refinement of the neutron data by the profile method gives an excellent fit with a reliability factor based upon point intensities,[9] R_{wpr}, of 4.4%. The derived structural parameters are in good agreement with those reported previously for $FePO_4$ and are given in Table I.

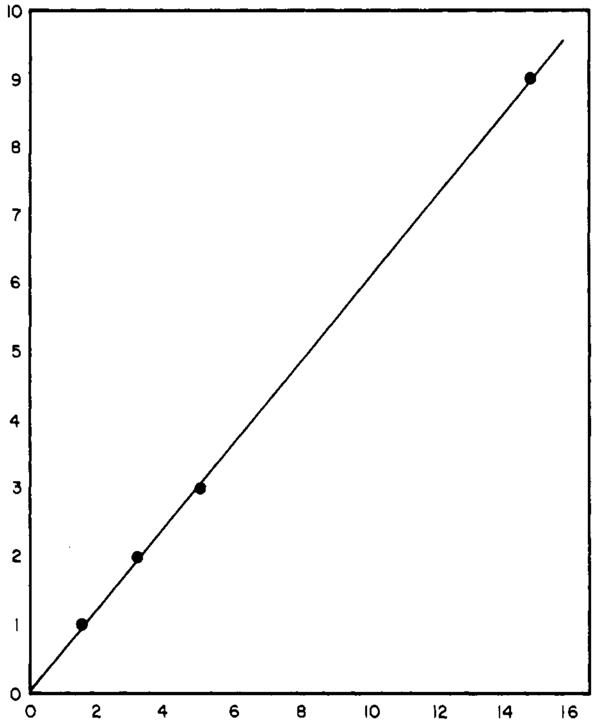

Figure 1. Plot of Fe Kα/P K$\alpha\beta$ ratio vs. Fe/P atomic ratio for several known materials.

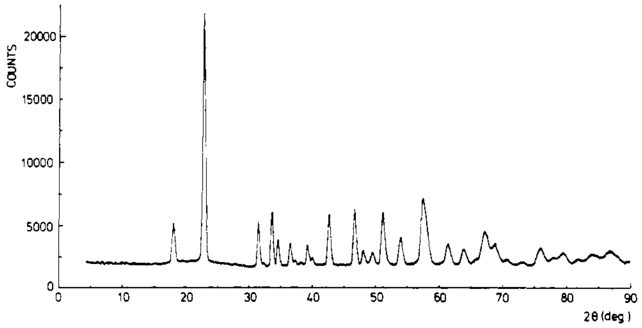

Figure 2. Powder neutron diffraction pattern observed for "$FePO_4$" at room temperature.

The first suggestion that the sample might not be pure came from the bulk chemical analysis by atomic absorption spectroscopy: found 33.0% Fe, calcd 37.0% Fe. Clearer evidence of a substantial impurity content was then found in the Mössbauer spectra obtained at temperatures between 300 and 1.5 K. Spectra measured above 30 K are essentially the same as that observed at 30 K and illustrated in Figure 3. Spectra obtained above 24.4 K require *three* quadrupole doublets for fitting and indicate that the material remains paramagnetic down to this temperature. The calculated Mössbauer-effect spectral data are presented in Table II, and the quality of the fits is illustrated in Figure 3. At 23.8 K the three paramagnetic

---

(7) Cheetham, A. K.; Skarnulis, A. J. *Anal. Chem.* **1981**, *53*, 1060.
(8) Cliff, G.; Lorimer, G. W. *J. Microsc.* (*Oxford*) **1975**, *103*, 203.
(9) Rietveld, H. M. *J. Appl. Crystallogr.* **1969**, *2*, 65.

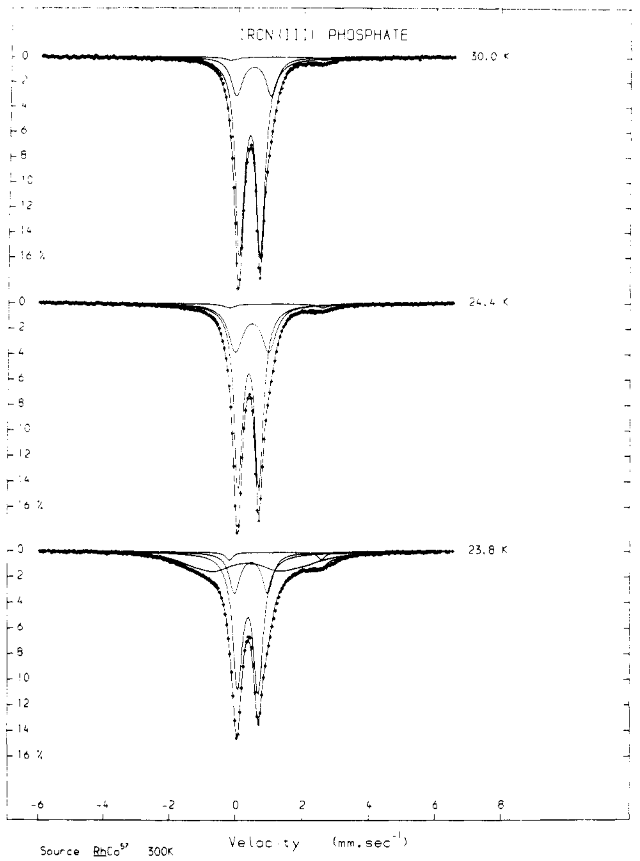

Figure 3. Mössbauer-effect spectra of "$FePO_4$" obtained at 30.0, 24.4, and 23.8 K.

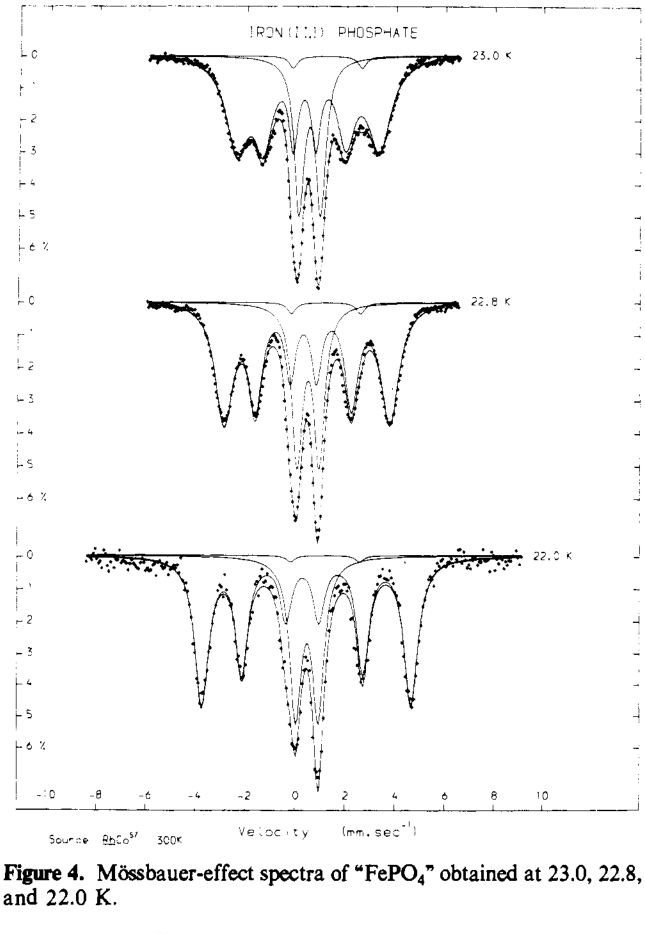

Figure 4. Mössbauer-effect spectra of "$FePO_4$" obtained at 23.0, 22.8, and 22.0 K.

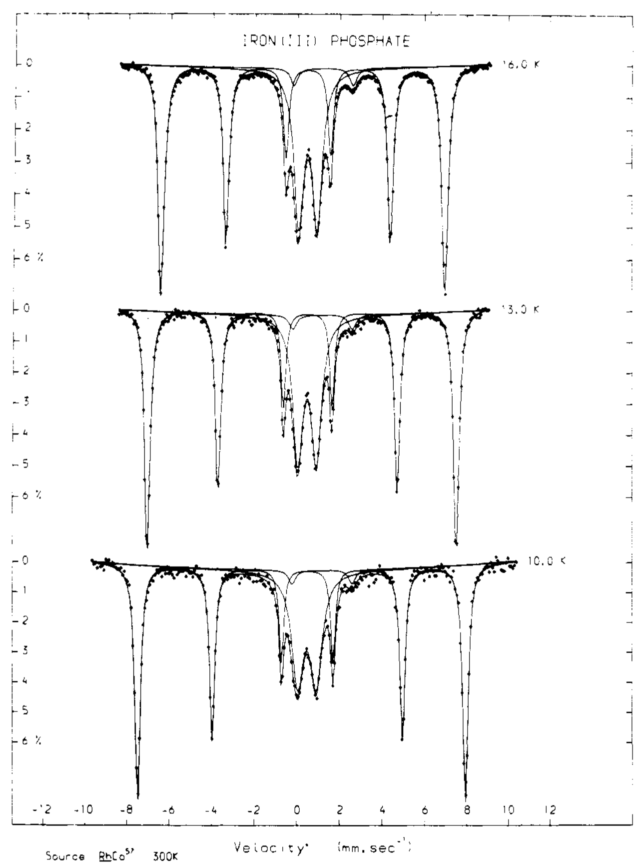

Figure 5. Mössbauer-effect spectra of "$FePO_4$" obtained at 16.0, 13.0, and 10.0 K.

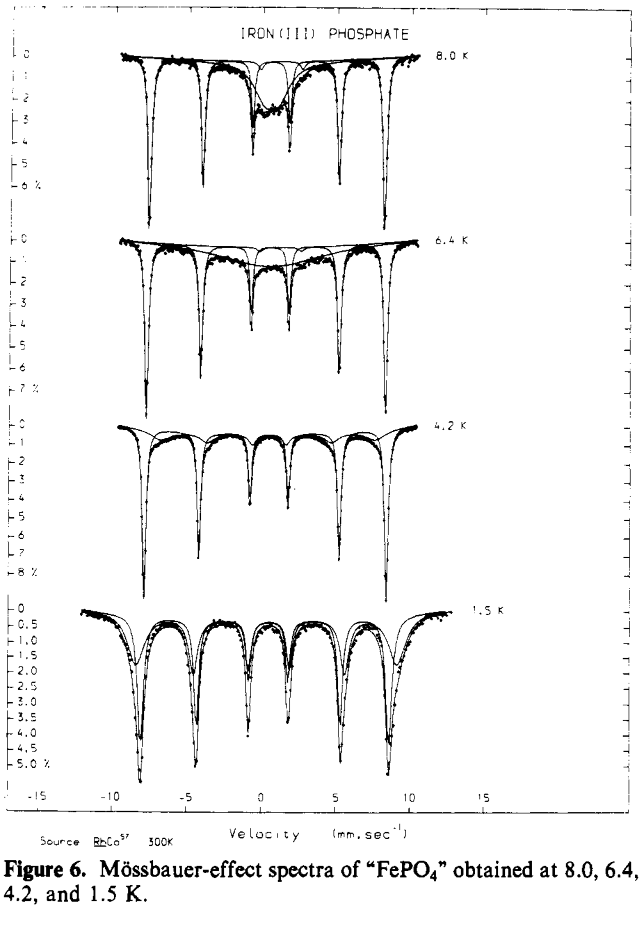

Figure 6. Mössbauer-effect spectra of "$FePO_4$" obtained at 8.0, 6.4, 4.2, and 1.5 K.

phases and 31% of an ordered phase of $FePO_4$ are observed (see Figure 3). Between 23.0 and 6.4 K, one magnetic sextet and two quadrupole doublets are needed, whereas below 6.4 K only two magnetic sextets are required. The results of these

Table III. Mössbauer-Effect Spectral Data for the Ordered Phase[a]

		FePO$_4$							Fe$_3$P$_5$O$_{17}$ (glassy component)							Fe$_7$(PO$_4$)$_6$			
T, K	H_{app}, T	H_{int}	δ	QS	Γ	$\Delta\Gamma$	$I_{2,5}$	%A	H_{int}	δ	Q[b]	Γ	$\Delta\Gamma$	$I_{2,5}$	%A	δ	ΔE_Q	Γ	%A
23.8		105	0.39	+0.04	1.00	1.43	4.00	31.3											
23.3		164	0.39	+0.07	0.59	0.75	1.66	73.7		0.50	0.91	0.52			25.5	1.20	2.77	0.40	2.2
23.0		177	0.37	+0.07	0.45	0.69	2.02	72.6		0.52	0.87	0.49			25.6	1.20	2.77	0.40	1.8
22.8		206	0.38	+0.07	0.50	0.39	1.84	71.9		0.51	0.88	0.52			27.5	1.20	2.77	0.40	1.6
22.0		260	0.38	+0.08	0.54	0.13	2.05	68.7		0.49	0.90	0.56			30.4	1.20	2.77	0.40	0.9
21.1		292	0.38	+0.08	0.56	0.06	2.24	69.3		0.48	0.93	0.57			29.7	1.20	2.77	0.40	0.9
18.7		363	0.38	+0.07	0.49	0.11	2.26	70.5		0.49	0.87	0.39			26.8	1.25	2.77	0.38	2.6
16.0		415	0.39	−0.13	0.30	0.06	2.11	64.9		0.50	0.87	0.56			32.4	1.21	2.89	0.37	2.7
13.0		450	0.38	−0.14	0.27	0.05	2.08	64.6		0.50	0.88	0.57			32.8	1.20	2.80	0.42	2.5
10.0		478	0.38	−0.14	0.26	0.05	2.02	65.8		0.51	0.87	0.67			31.8	1.21	2.79	0.38	2.4
8.0		490	0.38	−0.14	0.26	0.04	2.04	66.6		0.53	0.95	1.77			33.5	1.21	2.80	0.38	1.9
6.4		497	0.39	−0.14	0.25	0.05	2.14	64.5		0.53	1.75	5.89			33.7	1.20	2.80	0.40	1.8
4.2		503	0.38	−0.14	0.25	0.05	2.04	77.0	445	0.47	−0.06	0.53	1.02	1.82	23.0	*c*			
4.2	1	511	0.39	−0.15	0.29	0.10	1.97	85.1	434	0.43	−0.11	0.37	0.62	2.81	14.9	*c*			
4.2	2	511	0.39	−0.15	0.30	0.18	1.74	87.6	441	0.42	−0.11	0.20	0.77	3.36	12.4	*c*			
4.2	3	511	0.38	−0.13	0.33	0.15	1.44	80.9	441	0.44	−0.07	0.63	0.90	3.33	19.1	*c*			
4.2	4	510	0.39	−0.12	0.34	0.12	1.41	82.0	437	0.40	−0.11	0.30	0.78	3.61	18.0	*c*			
4.2	6	510	0.39	−0.11	0.34	0.09	1.33	78.9	444	0.43	−0.07	0.38	1.20	2.85	21.2	*c*			
1.65	4	510	0.39	−0.11	0.39	0.13	1.45	100.0	*c*							*c*			
1.50		517	0.39	−0.12	0.32	0.14	1.92	59.9	549	0.48	−0.08	0.54	0.87	1.82	40.5	*c*			

[a] Relative to room-temperature natural α-iron foil. All data in mm/s except H_{app} in kOe. [b] Q is the quadrupole interaction for paramagnetic spectra and the quadrupole shift for ordered spectra. [c] Component not observed.

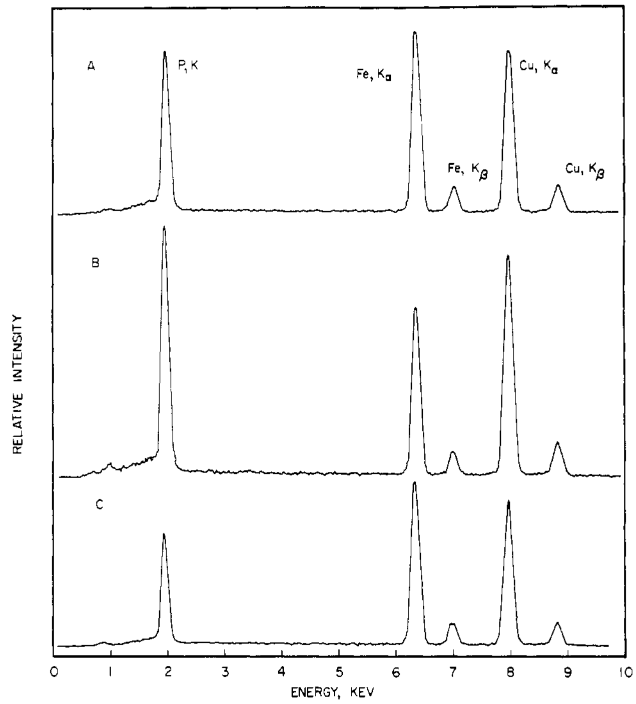

Figure 7. X-ray emission spectra of FePO$_4$ (A), the glassy Fe$_3$P$_5$O$_{17}$ (B), and Fe$_7$(PO$_4$)$_6$ (C), the three phases found in the "FePO$_4$", which was supported on a copper grid.

fits are illustrated in Figure 4–6, and the derived spectral parameters are given in Table III. Mössbauer spectra were also measured at 4.2 and 1.65 K in various transverse applied magnetic fields. The results obtained at 4.2 K indicate the presence of a second minor magnetic component which has essentially the same internal hyperfine field as the major component at 1.65 K and 4-T applied magnetic field. The derived parameters are presented in Table III. The Mössbauer results show clearly that the sample contains more than one phase. The results above 23.8 K (Table II) are consistent with two iron(III) components in the ratio of about 3.5:1 (based on Mössbauer-effect absorption areas) and a small quantity (approximately 2%) of the third component with parameters that are typical of octahedral high-spin iron(II). The onset of magnetic ordering at 23.8 K is due to the FePO$_4$ component,[3] and the second ordering transition between 8.0 and 6.4 K is associated with the smaller iron(III) component; a resolved magnetic hyperfine sextet for the latter phase is observed at 4.2 and 1.5 K (Figure 6). The Mössbauer-effect parameters derived for the ordered FePO$_4$ magnetic component show changes in the magnitude and sign of the quadrupole shift at 18 K, as found in pure FePO$_4$.[3] This change in the quadrupole shift corresponds to the spin-reorientation transition[3] in which there is a change in the angle between the axis of magnetization and the principal axis of the electric field gradient at the iron(III) nucleus. The hyperfine field saturates at a value of ca. 517 kOe at 1.5 K, in the range expected for a high-spin iron(III) ion with significant covalency in the iron–oxygen bond.[10]

The chemical composition of each of the impurity phases in our FePO$_4$ sample became clearer after a careful examination of the material by analytical electron microscopy. By this method, we were able to determine the Fe/P ratios of *individual* particles within the mixture. In addition to FePO$_4$, two other phases were detected (Figure 7). The first phase, with an Fe/P ratio of 0.59 (4), gave no electron diffraction pattern and appears to be a phosphate *glass* of the approximate

---

(10) Johnson, C. E. In "Hyperfine Interactions in Excited Nuclei"; Goldring, G., Kalish, R., Eds.; Gordon and Breach: New York, 1971; p 803.

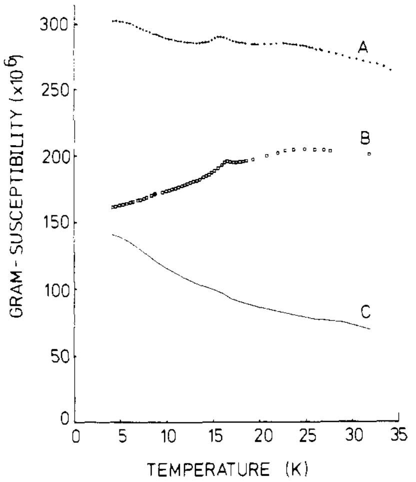

Figure 8. Gram magnetic susceptibility of "$FePO_4$" (A) and pure $FePO_4$ (B) and the difference in their susceptibility (C).

composition $Fe_3P_5O_{17}$. It is probably the same material as that previously reported as $Fe_4(P_2O_7)_3$ by d'Yvoire.[11] The latter material is apparently glassy[11] unless it is annealed at temperatures below 900 °C. The Mössbauer-effect parameters of our glassy component are clearly different from those of a $FePO_4$ glass for which an isomer shift of 0.31 mm/s and quadrupole interaction of 0.70 mm/s have been reported.[12] The larger isomer shift observed in $Fe_3P_5O_{17}$ is indicative of octahedral, rather than tetrahedral, iron(III) coordination. Below ca. 7 K, the glass is magnetically ordered, and the field dependence of its hyperfine spectrum is consistent with antiferromagnetic ordering. At 1.65 K and 4 T, both the glass and $FePO_4$ saturate to approximately the same internal hyperfine field.

The second impurity revealed by microanalysis has an Fe/P ratio of 1.17 (1) and is almost certainly the mixed valence compound[13] $Fe_3^{II}Fe_4^{III}(PO_4)_6$, with Fe/P = 1.167. Only the iron(II) present in this phase is observed in the Mössbauer spectra, and its Mössbauer-effect parameters are in good agreement with those found by Gleitzer ($\delta = 1.12$ mm/s; $\Delta E_Q = 2.56$ mm/s for an authentic sample of $Fe_3^{II}Fe_4^{III}(PO_4)_6$).[14] The iron(III) resonance from this phase is probably hidden within the absorption from $FePO_4$ and the glass. It is known[14] that $Fe_7(PO_4)_6$ is paramagnetic down to ca. 100 K; the Mössbauer spectra indicate that it remains paramagnetic down to at least 10 K, as observed in Figure 5. The presence of a mixed valence impurity is surprising considering the oxidizing conditions to which the sample was subjected, but the stability of this phase is so great that it is a common impurity under these conditions.[14]

The gram magnetic susceptibility of our $FePO_4$ sample is shown as plot A in Figure 8. Most of the features found for pure $FePO_4$ (plot B in Figure 8) can be seen in the triphasic mixture, and we can now calculate the magnetic susceptibility curve for the glassy component (plot C, Figure 8); the contribution of the mixed valence component to the susceptibility is apparently negligible. The results in plot C of Figure 8 again indicate antiferromagnetic ordering in the glass below ca. 6 K.

Conclusions

The results of this work underline the difficulties that can arise when materials are characterized solely by powder diffraction methods in which the presence of a glassy impurity can be completely overlooked. With the knowledge of hindsight, we can see some diffuse scattering from the glass in the neutron pattern at a 2θ value of approximately 23°. Equally, our work has shown that a good deal can be learned about polyphasic materials, even those containing glassy components, when a combination of physical methods is used. In particular, the use of analytical electron microscopy is a powerful approach, yielding information about both composition and crystallinity. Together with the Mössbauer effect and magnetic susceptibility results, it has enabled us to present a detailed picture of a complex mixture.

Acknowledgment. P.D.B. is grateful to the Central Electricity Generating Board and St. Catherine's College, Oxford University, for the award of a Research Fellowship. We also thank the SERC for the provision of neutron facilities (Grant GR/B37196) and a grant toward the purchase of an analyical electron microscope (GR/A3320) and NATO for a cooperative scientific research grant.

Registry No. $FePO_4$, 10045-86-0; $Fe_7(PO_4)_6$, 78357-26-3; Fe, 7439-89-6; H_3PO_4, 7664-38-2.

---

(11) d'Yvoire, F. *Bull. Soc. Chim. Fr.* **1962**, 1224.

(12) Kurkijian, C. R.; Sigety, E. A. *Phys. Chem. Glasses* **1968**, *9*, 73.

(13) Gorbunow, U. A.; Maksimov, B. A.; Kabatov, U. K.; Evachenko, A. N.; Mielnikov, O. K.; Bietov, N. B. *Dokl. Akad. Nauk SSSR* **1980**, *254*, 873.

(14) Gleitzer, C., unpublished results.